Chem. Res. Chin. Univ., 2018, 34(4), 676—683 doi: 10.1007/s40242-018-8077-2

Light-stimulus Dual-drug Responsive Nanoparticles for Photoactivated Therapy Using Mesoporous Silica Nanospheres

WU Peng[1], ZHOU Dongfang[2], HUANG Yubin[2] and LI Jizhen[1*]

1. College of Chemistry, Jilin University, Changchun 130021, P. R. China;

2. State Key Laboratory of Polymer Physics and Chemistry, Changchun Institute of Applied Chemistry, Chinese Academy of Sciences, Changchun 130022, P. R. China

Abstract Photoactivated therapy is an exciting new method of cancer treatment. A new light-stimulus dual-drug responsive nanoparticles based on mesoporous silica nanoparticles(MSN) were developed to control cellular anticancer drug release. The prepared Curcumin(Cur)-loaded nanoparticles MSN-Pt-PEG@Cur[PEG=poly(ethylene glycol)] could be activated by photostimulation to generate reactive oxygen species(ROS) from Cur and Pt(II) from Pt(IV), respectively. Compared with free anti-cancer drugs' chemotherapy and single photoactivated therapy, the prepared MSN-Pt-PEG@Cur displayed increased cytotoxicity. Therefore, the strategy of light-stimulus dual-drug responsive nanoparticles is a promising approach to photoactivated therapy.

Keywords Photoactivated therapy; Dual-drug nanoparticle; Curcumin; Platinum

1 Introduction

Over the past few decades, the use of controlled drug delivery systems(CDDS) has been explored widely in the anti-cancer field[1]. Liposomes, dendrimers, polymer nanoparticles, inorganic-organic hybrid nanoparticles and inorganic nanomaterials have been used as nanocarriers to improve efficiency and reduce toxicity[2]. Among them, mesoporous silica nanoparticles(MSNs) have several advantages, such as nontoxicity, pore size adjustability, good biocompatibility, high large surface area and ease to modify[3—6]. For the treatment of tumors, MSNs have been prepared to load various anticancer drugs[7]. Some of these formulations showed excellent results in controlled drug release and improved curative effect[8,9]. Because of tumor heterogeneity, a single stimuli-responsive therapy is typically not sufficient[10]. Photoactivated therapy[11] is a supplemental and promising method for tumor chemotherapy, offers noninvasiveness, precise control, site selectivity, and is easily regulated by light. Modern photoactivated therapy involves photodynamic therapy(PDT)[12—16], photo chemotherapy(PCT)[13], and photo-thermal therapy(PTT)[14]. The use of photosensitizer(PS)[17] can generate reactive oxygen species (ROS) for PDT within a remarkably short time(<40 ns) to produce instantaneous cellular damage. Photoactivated metal chemotherapeutic drug(PCD)[18] can release active chemotherapeutic drugs in sustained manner for PCT. Thus, a tumor therapy strategy consisting of rapid PDT and long-lasting PCT potentially would be more effective.

Many compounds including chemicals, antineoplastic agents, and dyes with photosensitive properties have been proposed for use in photoactivated therapy[19,20]. Curcumin (Cur)[21], a traditional Chinese medicine with anti-cancer activity, has been utilized as an effective PS. However, Cur has low solubility and exhibits instability in an aqueous environment, limiting its clinical application. Platinum(II)[Pt(II)] complexes have been applied as effective anti-cancer chemotherapeutic agents. However, clinical use of these complexes is accompanied with acquired resistance and severe systemic toxicity[22]. Sadler *et al.*[23] reported various photoactivated Pt(IV)-N_3 compounds, which as PCD could maintain stability under dark condition and could be selectively photoactivated in tumor tissue by photostimulation.

Our previous researches focused on drug loading and release of nano-systems[7,11,14,16,24]. We considered that Pt(py) [a Pt(IV)-N_3 compound] could function as a PCD if it was linked to the surface of MSN. And then encapsulating the Cur into nanoparticles would allow the construction of a dual-drug response model to kill tumor cells. Cur can be photoactivated by light to induce ROS generation in cancer cells for rapid PDT. Pt(py) can also be photoactivated to release active Pt(II) for long-lasting PCT. In this work, as shown in Scheme 1, we demonstrated a new light stimulus dual-drug responsive nanoparticles to co-release Curcumin and Pt(py) for combinational photoactivated treatment. The photoactivated antitumor effect of these nanoparticles was assessed.

*Corresponding author. Email: ljz@jlu.edu.cn

Received March 12, 2018; accepted May 5, 2018.

Supported by the National Natural Science Foundation of China(No.51573069) and the Project of the Department of Science & Technology of Jilin Province, China(No.20170414052GH).

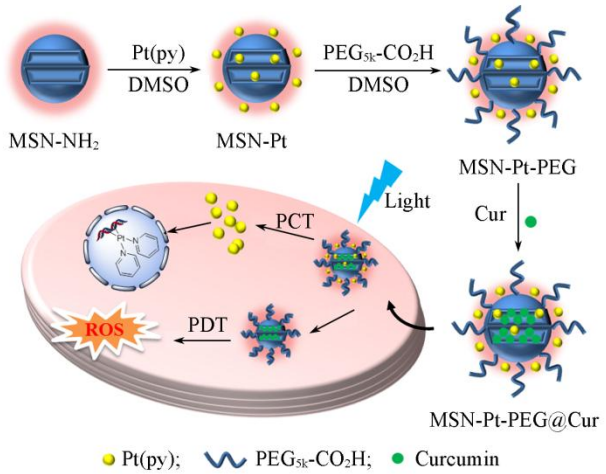

Scheme 1 Schematic diagram of Pt(II) and Cur released from MSN-Pt-PEG@Cur for combinational photoactivated therapy

2 Experimental

2.1 Materials

Cisplatin(99%) and Cur(99%) were purchased from Shandong Boyuan Chemical Company and Sinopharm Chemical Reagent Limited Company, respectively. Propargylamine, (3-chloropropyl) trimethoxysilane, poly(ethylene glycol) monomethyl ether($mPEG_{5k}$), and 3-aminopropyl trimethoxysilane(APTES) were purchased from Sigma. 3-(4,5-Dimethylthiazol-2-yl)-2,5-diphenyl-tetrazolium bromide(MTT) and Hoechst nuclear dye were purchased from Sigma-Aldrich. *N*-Cetyl-trimethyl-ammonium bromide(CTAB) and dichlorodihydro-fluorescein diachetate(DCF-DA) were bought from Yili Fine Chemicals Co., Ltd., Beijing, China and Biyuntian Biological Co., Ltd., Shanghai, China, respectively. Tetraethyl orthosilicate(TEOS), 1-ethyl-3-[3-dimethylaminopropyl]carbodiimide hydrochloride(EDC HCl), and *N*-hydroxysuccinimide (NHS) were purchased from Aladdin.

2.2 Synthesis of Pt(py)

The starting material complex of *trans*,*trans*,*trans*-$[Pt(N_3)_2(OH)_2(py)_2]$ was synthesized according to the published procedure[23]. *Trans*,*trans*,*trans*-$[Pt(N_3)_2(OH)_2(py)_2]$(1.0 g, 2.1 mmol) and succinic anhydride(255 mg, 2.54 mmol) were dissolved in 5 mL of dry DMSO under nitrogen, followed by stirring at 60 °C for 24 h. The mixture was pumped under vacuum, then dissolved in methanol and settled by ether. The final product Pt(py) was isolated by filter and vacuum drying(Scheme 2).

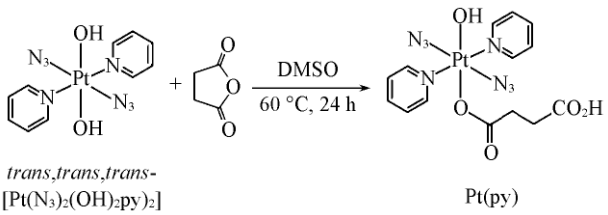

trans,*trans*,*trans*-$[Pt(N_3)_2(OH)_2py)_2]$ Pt(py)

Scheme 2 Synthesis route of Pt(py)

Pt(py): yellow powder, 75% yield. ^{1}H NMR(400 MHz, DMSO), δ: 8.79(m, 4H), 8.28(m, 2H), 7.73(m, 4H), 2.47—2.41 (t, J=6.8 Hz, 2H), 2.39—2.32(t, J=6.4 Hz, 2H). MS(ESI), *m/z*: calculated for $C_{14}H_{15}N_8O_5Pt[M–H]^+$: 570.1, found: 570.2 (Fig.S1, see the Electronic Supplementary Material of this paper). The data were completely in agreement with those in the published reference[25].

2.3 Preparation of MSN-Pt-PEG@Cur

$MSN-NH_2$ was synthesized as described in ref.[25]. CTAB(0.5 g) was dissolved in distilled water(500 mL) within NaOH(1.75 mL, 2 mol/L) at 80 °C. Then TEOS(2.5 mL) was dripped into the mixed liquor and kept mechanical rabbling for 2 h. The sediment was separated by centrifugation(12000 r/min), washed with ethanol and deionized, then dried. The obtained white powder and APTES(0.5 mL) were added to dry toluene under nitrogen, then stirred for 24 h at 90 °C. The precipitation was collected, and then washed with water and ethanol. The sample was then dispersed in methanol(150 mL) containing HCl(9 mL, 98%), under reflux conditions for 10 h to eliminate the CTAB. The precipitation was purified by centrifugation and washed with ethanol. In the end, the $MSN-NH_2$ containing amino groups were obtained.

$MSN-NH_2$(250 mg) was ultrasonic dispersed into dry DMSO(5 mL) under nitrogen, then the dissolved DMSO solution of Pt(py)(250 mg, 0.44 mmol), EDC HCl(394 mg, 2.2 mmol), and NHS(253 mg, 2.2 mmol) was injected into the above dispersion liquid, stirred at room temperature for 72 h. MSN-Pt was collected after centrifugation, washed with water and dried under vacuum. MSN-Pt-PEG was similarly synthesized according to the above procedure. MSN-Pt(250 mg), PEG_{5k}-CO_2H(1.0 g, 0.2 mmol), EDC HCl(180 mg, 1.0 mmol), and NHS(115 mg, 1.0 mmol) were dissolved in 5 mL of dry DMSO and kept for 72 h. The MSN-Pt-PEG was acquired as a yellow powder after centrifugation, washed with water, and dried under vacuum.

The loading of Cur was performed according to our previous reported method[24], using an m(MSN):m(Cur)=10:1. In detail, MSN-Pt-PEG(200 mg) and Cur(20 mg) were dissolved in DMSO(5 mL), and then stirred for 24 h. The mixture was centrifuged(12000 r/min) for 10 min. Finally, the Cur-loaded material was repeatedly washed with ethanol and dried under vacuum. A typical measurement of the Cur-ethanol solutions showed that the drug loading content and efficiency were 8.3% and 90%, respectively. The drug loading content(DLC) was calculated as below:

$$\mathrm{DLC}(\%) = \frac{\text{Mass of Cur in particles}}{\text{Total mass of particles}} \times 100\% \quad (1)$$

2.4 *In vitro* Assays

2.4.1 *Photosensitivity of MSN-Pt-PEG@Cur*

An aqueous solution of MSN-Pt-PEG@Cur was irradiated under a range of wavelengths(365, 430 and 530 nm under 20 mW/cm^2) for a set time and then the UV-Vis spectra were recorded. Continuous irradiation and periodic irradiation were separately used to assess the photosensitivity.

2.4.2 Photo-triggered Drug Release

MSN-Pt-PEG@Cur particles(3.0 mg) were dissolved in 1.0 mL of acetate buffer solution(pH=5.0) or phosphate buffer(pH=7.4). The solution was immersed in a dialysis tube(molecular weight cut-off=3500), and placed into the buffer solution(19 mL), followed by putting into concussion incubator at 37 °C. The solution was monitored in the dark or under continuous or periodic light(365, 430 and 530 nm under 20 mW/cm^2). For each sample, a 3.0 mL of aliquot of buffer solution outside the dialysis tube was removed at preset time to record the UV-Vis spectra.

2.4.3 Cellular Uptake

Endocytosis and intracellular drug release of MSN-Pt-PEG@Cur were measured on a confocal laser scanning microscopy(CLSM) using Skov-3 cells. The cells were placed into a 6-well culture tray(5×10^4 cells each hole) and cultured for 12 h. After 12 h, the cells were treated with MSN-Pt-PEG@Cur or free Cur at a Cur concentration of 3.0 μg/mL for 4 h at 37 ℃. Then, after the removal of medium, the Skov-3 cells were washed with PBS and fixed with 4% formaldehyde for 15 min. Finally, the nuclei were stained by Hoechst. Fluorescence was monitored by a CLSM image system.

2.4.4 Detection of Intracellular ROS

The amount of ROS generated in cells was detected by DCF-DA(a cellular ROS labeling reagent). Skov-3 cells were placed into a 6-well culture tray(5×10^4 cells each hole), pre-incubated in an incubator overnight. Then the culture solution was replaced with MSN-Pt-PEG@Cur(Cur, 3.0 μg /mL) or Cur(3.0 μg/mL). Two treatments were performed: the cells were cultured for 4 h in the dark; or the cells were incubated with Cur and MSN-Pt-PEG@Cur and exposed to illumination (530 nm, 20 mW/cm^2) for 30 min. After treatment, the culture solutions were then changed for 1.0 mL of 1640 serum-free including 1.0 μL of DCFH-DA. The cells were cultured for another 30 min, then washed multiple times with PBS. The fluorescence photos of all groups were observed by the CLSM image system.

2.4.5 Cell Cytotoxicity

Cytotoxicity was evaluated by MTT assay. The Skov-3 cells were seeded into a 96-well culture tray(5×10^3 cells each hole), pre-incubated in an incubator for 24 h. The cells were incubated with Cisplatin, Pt(py), Cur, MSN-Pt-PEG@Cur(mass fraction: Cur: 8.3%, Pt 11.2%) at a Pt gradient concentration of 3.375—216 μmol/L or a Cur gradient concentration of 0.5—24 μg for 4 h. Next, the cells were washed with PBS and then cultured for another 72 h with fresh 1640 medium. Cells in the light treatment groups were exposed to irradiation(530 nm, 20 mW/cm^2) for 30 min after 4 h endocytosis. Fresh 1640 medium without drugs was then used to replace the media and cells were then cultured in the dark. After 72 h, all groups were stained with 20 μL of MTT(0.5 mg/mL), and co-cultured for 4 h. This was followed by the addition of 150 μL of DMSO to all wells. The culture tray was vibrated for 5 min, and the spectrometric absorbance was determined by microplate reader.

2.4.6 Combination Index(CI) Analysis

The combination index(CI) was calculated using the formula described below, providing qualitative interactive drug relationship information. $c_{A,x}$ is the concentration of drug A[Pt(py)] and $c_{B,x}$ is the concentration drug B(Cur). These two drugs were applied in a combined treatment to attain x% drug toxicity. $IC_{x,A}$ and $IC_{x,B}$ are the concentrations for each single treatment required to attain the same drug toxicity.

$$CI = \frac{c_{A,x}}{IC_{x,A}} + \frac{c_{B,x}}{IC_{x,B}} \quad (2)$$

3 Results and Discussion

3.1 Characterization of MSN-Pt-PEG@Cur

The prepared mesoporous silica particles MSN-NH_2 were characterized by the determination of BET nitrogen adsorption-desorption isotherms and BJH pore size distribution analysis. As shown in Fig.1(A), the BET isotherm of MSN-NH_2 reveals the IV type of N_2 adsorption-desorption model based on the IUPAC rules, indicating that the nanoparticles are ordered spherical and exhibits a low pore size distribution. The corresponding specific surface area was calculated as 994.8 m^2/g and the mean pore size was 3.46 nm[Fig.1(B)]. The measurement of three characteristic peaks at (100), (110) and (200) by low-angle X-ray diffraction(XRD) was consistent with the MCM-41 type of MSN-NH_2 mesoporous silica[Fig.1(C) and Fig.S2, see the Electronic Supplementary Material of this paper]. Together, these data indicate MSN-NH_2 with mesoporous property was successfully prepared.

Prepared photosensitive prodrug Pt(py) and PEG_{5k}-COOH grafted to the particles were characterized as shown in Fig.2.

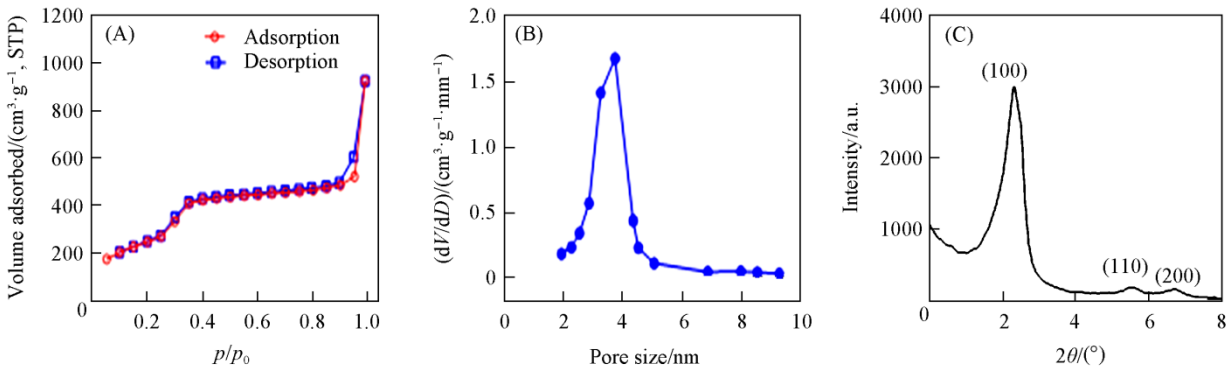

Fig.1 BET isotherms(A), BJH pore size distribution(B) and XRD pattern(C) of MSN-NH_2

The infrared spectra[Fig.2(A)] reveal that the characteristic peak of —N_3 at 2061 cm^{-1} appears in MSN-Pt-PEG. The carbonyl peak at 1725 cm^{-1} disappears and the peak at 1663 cm^{-1} appears, revealing the successful transformation from chemical group —COOH to —CONH. Furthermore, a new absorption peak appeared at 1440 cm^{-1} can be ascribed to the C—H bonds in PEG. These data indicate that Pt(py) and PEG were successfully linked to MSN-NH_2. Compared to the cloudy aqueous solution of MSN-NH_2, the MSN-Pt-PEG and MSN-Pt-PEG@Cur solutions are clear and transparent, also indirectly confirming the successful grafting of PEG[Fig.2(B)]. The Cur-loaded nanoparticles were monitored by the normalized absorbance spectra(Fig.3). Characteristic absorption peak of —N_3 at 298 nm can be observed in MSN-Pt-PEG and the characteristic absorption peak of Cur appears at 439 nm in Cur-loaded particles, showing that Cur was loaded in the MSN-Pt-PEG particles.

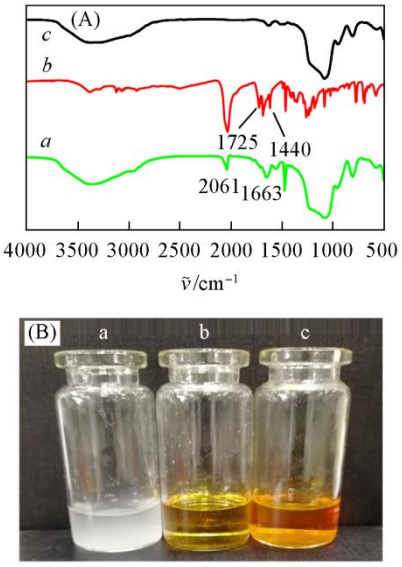

Fig.2 FTIR spectra(A) of MSN-Pt-PEG(*a*), Pt(py)(*b*) and MSN-NH_2(*c*) and photos(B) of MSN-NH_2(a), MSN-Pt-PEG(b) and MSN-Pt-PEG@Cur(c) dissolved in water

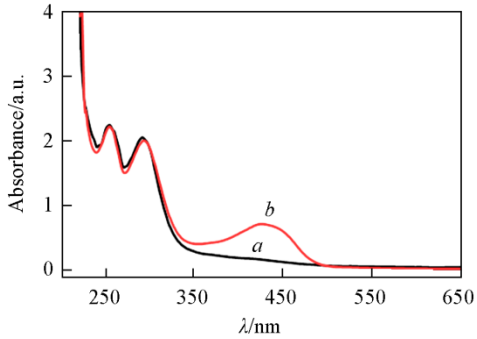

Fig.3 UV-Vis spectra of MSN-Pt-PEG(*a*) and MSN-Pt-PEG@Cur(*b*)

The size and morphology of the nanoparticles were characterized by dynamic light scatter(DLS) and transmission electron microscopy(TEM). The DLS data indicate that the diameter of unmodified MSN-NH_2 is approximately 100 nm (Fig.4). After modification, the diameters are slightly increased. Owing to the good dispersibility of MSN-Pt-PEG@Cur in aqueous solution, the diameter of MSN-Pt-PEG@Cur is approximately 230 nm, larger than that measured in TEM. The morphologies of MSN-NH_2 after modification were observed using TEM. The pictures in Fig.5(A) indicate the uniform morphologies of the prepared MSN-NH_2 particles. However, the surface of nanoparticles becomes crude and a shell could be observed clearly after Pt(py) and PEG grafting [Fig.5(B) and (C)].

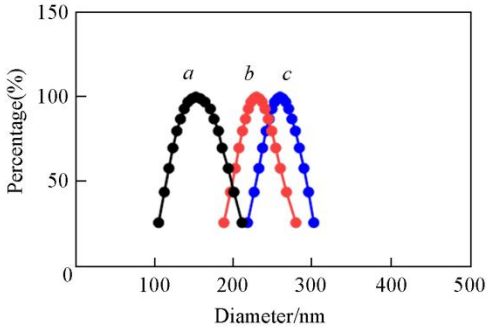

Fig.4 Hydrodynamic diameter distribution of MSN(*a*), MSN-Pt-PEG(*b*) and MSN-Pt-PEG@Cur(*c*)

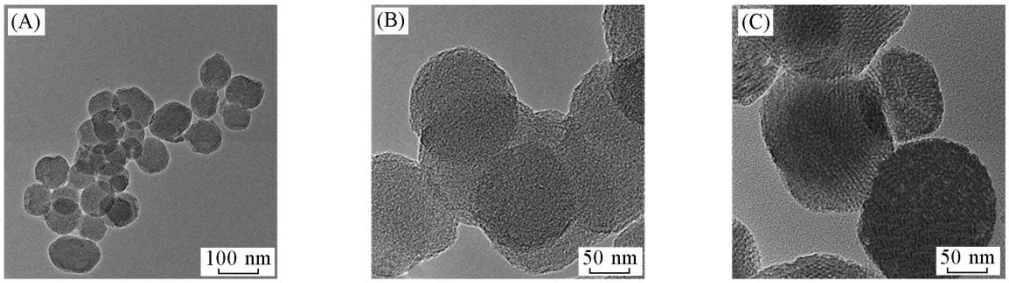

Fig.5 TEM images of MSN-NH_2(A), MSN-Pt-PEG(B) and MSN-Pt-PEG@Cur(C)

3.2 Photosensitivity of MSN-Pt-PEG@Cur

As a photosensitizer, Cur exerted anti-tumor effect along with ROS generation when irradiated by UV or visible light. As a PCD, Pt(py) could be selectively activated by multi-wavelength light(from UV to visible light) to release the cytotoxic Pt(II).

In order to explore the photosensitivity of these two drugs, we used light irradiation with different wavelengths(365, 430 and 530 nm under 20 mW/cm^2) to irradiate MSN-Pt-PEG@Cur and recorded the change of their UV-Vis spectra. As shown in Fig.6(A)—(C), both Cur and photosensitive Pt(py) show rapid response under these light conditions. The peaks of

MSN-Pt-PEG@Cur at 298 and 439 nm decrease simultaneously upon exposure to light. We noted that the absorbance of Pt-N_3 under 530 nm light dropped more slowly than that upon 365 nm irradiation. According to the photolysis curves, the photoreduction rates were in a definite sequence of 365 nm> 430 nm>530 nm. Performed the indirect light stimulation to MSN-Pt-PEG@Cur, the peak change of the —N_3 peak at 298 nm shows an 'on-off' effect. Correspondingly, the rate of descent was accelerated when particles were exposed to light, with no change under dark conditions[Fig.6(D)].

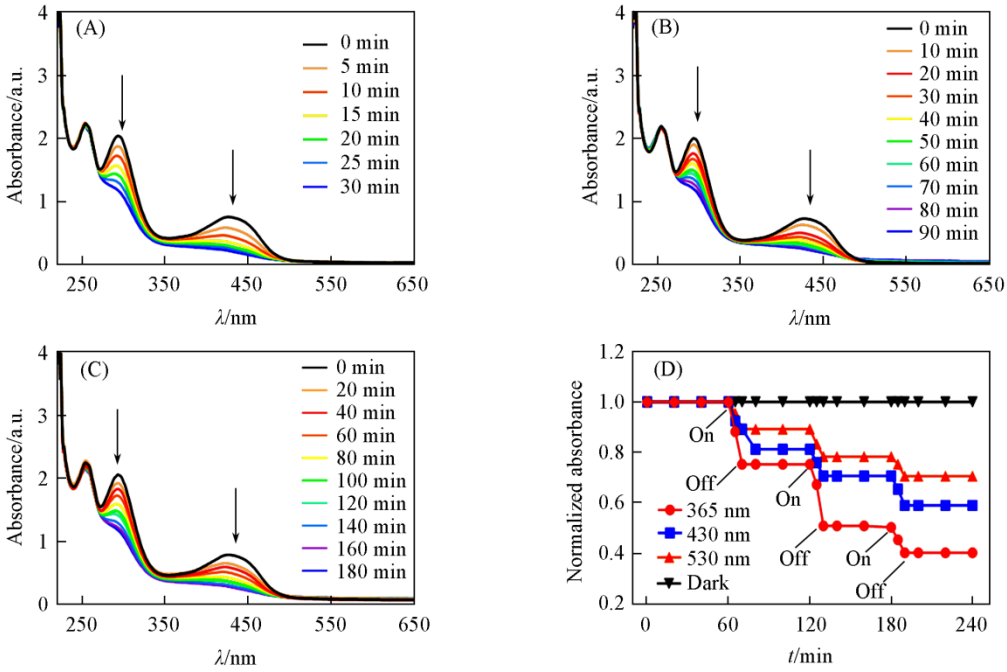

Fig.6 UV-Vis spectra of MSN-Pt-PEG@Cur upon light irradiation(20 mW/cm^2) with wavelengths of 365(A), 430(B) and 530 nm(C) for different periods of time and normalized UV absorption of MSN-Pt-PEG@Cur at 298 nm under intermittent irradiation(365, 430 and 530 nm, 20 mW/cm^2)(D)

3.3 Cur and Pt(py) Loading and Release

Cur can be loaded into nanoparticle through hydrophobic interaction. The Cur loading content of particles was 8.3%. To study the release of platinum and Cur, MSN-Pt-PEG@Cur was subjected to a dialysis method under dark or light irradiation (365, 430 and 530 nm, 20 mW/cm^2 at pH=7.4). As shown in Fig.7, both Pt and Cur show some release under dark, but

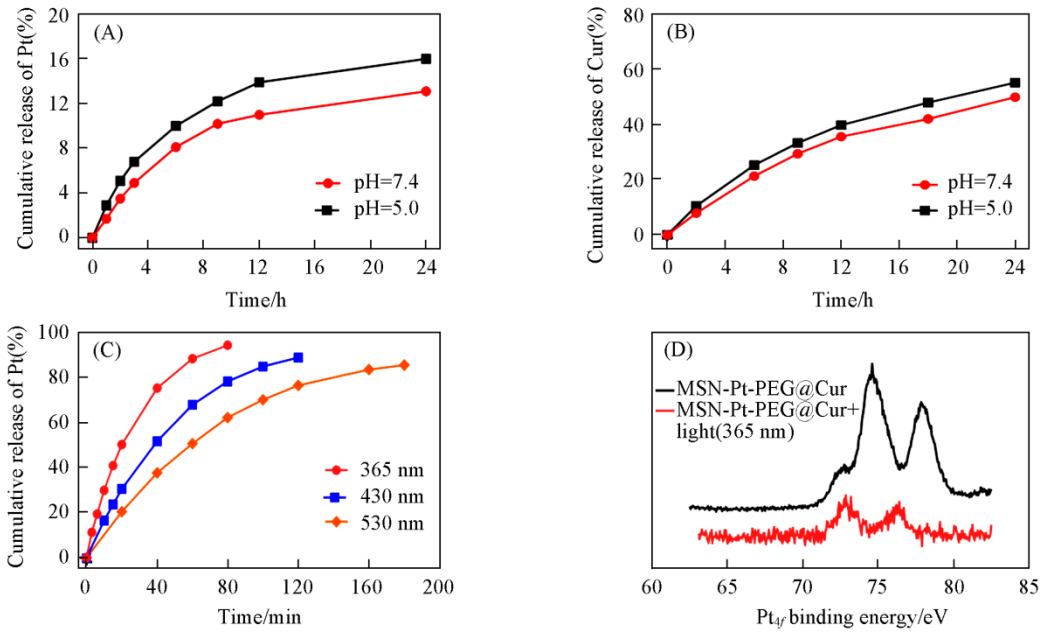

Fig.7 Pt(A) and Cur(B) release profiles of MSN-Pt-PEG@Cur under dark, Pt release profiles of MSN-Pt-PEG@Cur in water under light detected by ICP-OES(C) and XPS spectra change of MSN-Pt-PEG@Cur under irradiation(365 nm, 20 mW/cm^2) for 1 h(D)

their release rates at pH of 5.0 are faster than that at pH of 7.4[Fig.7(A), (B)]. The Pt release was continuously accelerated upon continuous irradiation, and Pt almost released completely within 90 min under 365 nm. In addition, it took only 3 h to reach the Pt release maximum value at 530 nm[Fig.7(C)]. The oxidation state of Pt in MSN-Pt-PEG@Cur before and after irradiation was next determined by X-ray photoelectron spectroscopy(XPS), as shown in Fig.7(D). Pt_{4f} in MSN-Pt-PEG@Cur exhibits the characteristic binding energies(77.9 and 74.6 eV) of Pt(IV) in the absence of light, but after irradiation(365 nm) for 1 h, the binding energies are 76.4 and 72.8 eV. The above results indicate that the Pt(py) in MSN-Pt-PEG@Cur was transferred to active Pt(II) complex upon irradiation.

3.4 Cellular Uptake and ROS Generation of MSN-Pt-PEG@Cur

CLSM was used to observe the intracellular uptake of MSN-Pt-PEG@Cur. Skov-3 cells were incubated with MSN-Pt-PEG@Cur or Cur alone. The nuclei were stained by Hoechst(blue fluorescence). As shown in Fig.8, both Cur and MSN-Pt-PEG@Cur were detected in the cytoplasm(as evident by green fluorescence) after 4 h of incubation. However, the green fluorescence also appeared in nuclei incubated with Cur alone, indicating that particles were successfully captured by the cells instead of being released only by diffusion.

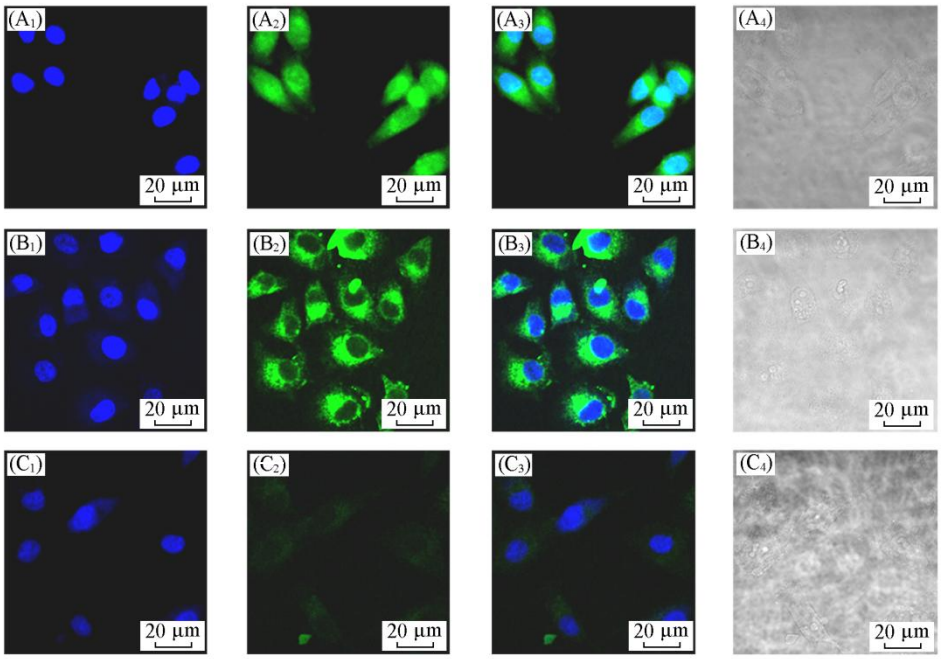

Fig.8 CLSM photos of Skov-3 cells incubated for 4 h with Cur(A_1—A_4) and MSN-Pt-PEG@Cur(B_1—B_4) and control group in dark(C_1—C_4)

(A_1)—(C_1) Hoechst; (A_2)—(C_2) 488 nm; (A_3)—(C_3) merged; (A_4)—(C_4) brightfield.

To assess the ROS generation of MSN-Pt-PEG@Cur, dichlorofluorescein diacetate(DCF-DA) was used to indicate ROS after cell internalization upon irradiation. Hyperfluorescence is produced by the rapid oxidization of DCF-DA when the ROS is present. As shown in Fig.9, because the cell itself contains a little of ROS, a low level of fluorescence can be

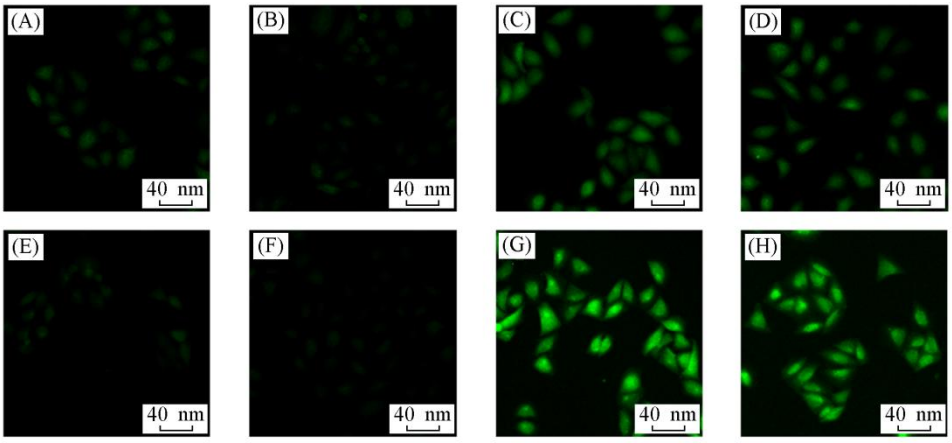

Fig.9 CLSM photos of Skov-3 cells treated in the dark(A—D) or under irradiation(E—H) with control+DCF-DA(A, E), Cur+DCF-DA(–)(B, F), Cur+DCF-DA(+)(C, G) and MSN-Pt-PEG@ Cur+DCF-DA (+) (D, H)

observed in the control groups[Fig.9(A), (E)] and the blank groups[Fig.9(B), (F)]. The fluorescence of the control groups show little change under dark or exposed to light. The cells treated with Cur and MSN-Pt-PEG@Cur with DCF-DA in the dark also express weak fluorescenc[Fig.9(C), (D)]. Conversely, due to the substantial ROS generation, green hyperfluorescence can be observed in both Cur and MSN-Pt-PEG@Cur treated groups after irradiation for 30 min(530 nm, 20 mW/cm^2) [Fig.9(G), (H)]. There is little fluorescence from Cur and MSN-Pt-PEG@Cur without light, indicating that the improved fluorescence appeared in the light treatment group can be due to the increased ROS. Concisely, MSN-Pt-PEG@Cur rapidly generated ROS for effective PDT.

3.5 Cytotoxicity Study *In vitro*

To study the anticancer activity of MSN-Pt-PEG@Cur, Skov-3 cancer cells were used and the MTT assay was performed(Fig.10 and Fig.S3, see the Electronic Supplementary Material of this paper). The cells were treated with Cur, Cisplatin and Pt(py)(as control). The cell viability of Skov-3 treated with Cur-loaded nanoparticles and free Cur was evaluated. In the dark, Cur and photosensitive Pt(py) exhibited minimal cytotoxicity and MSN-Pt-PEG@Cur showed comparatively low cytotoxicity. There were significant changes of cytotoxicity after irradiation for 30 min(530 nm, 20 mW/cm^2) with MSN-Pt-PEG@Cur. The cytotoxicity of MSN-Pt-PEG@Cur against Skov-3 cells was about 7-fold upon irradiation than without light, with better anti-cancer capability than Cur or Pt(py)[Fig.11(A), (B)]. The results imply that the cell toxicity of the dual responsive nanoparticles could be effectively controlled by photostimulation.

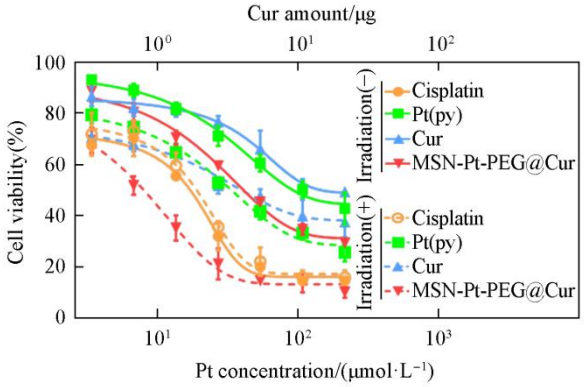

Fig.10 Cytotoxicity curves *in vitro* against Skov-3 cells treated with different drugs for 72 h

To investigate the synergy of combinational photoactivated anti-cancer therapy, CI determination was carried out. Pt(py) and Cur were tested as single drug therapy system, whereas MSN-Pt-PEG@Cur was selected as corresponding combinational system. Normally, the CI values are less than, equal to, or greater than 1.0, denoting synergy, additive property, or antagonism, respectively. As shown in Fig.12, the measured CI values are plotted against drug effect levels(IC_x values, *e.g.*, IC_{50}), and all CI values of the MSN-Pt-PEG@Cur are less than 1.0, suggesting the synergy of Cur for PDT and Pt(py) for PCT in combinational therapy against Skov-3 cells. In conclusion, the results indicate that MSN-Pt-PEG@Cur might be effective light-stimulus dual-drug responsive nanoparticles against Skov-3 ovarian cancer cells for use in improved photoactivated therapy with a combination of PDT and PCT.

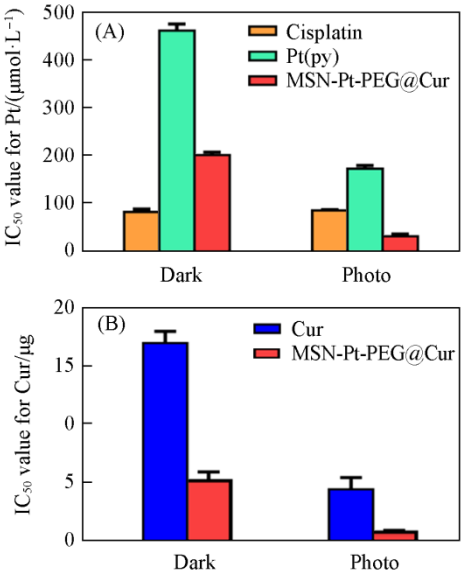

Fig.11 IC_{50} values of Cisplatin(Pt, μmol/L), Pt(py)(Pt, μmol/L), MSN-Pt-PEG@Cur(Pt, μmol/L; Cur, μg), and Cur(Cur, μg) against Skov-3 cells after 72 h of incubation in the dark or with light

(A) For Pt; (B) for Cur.

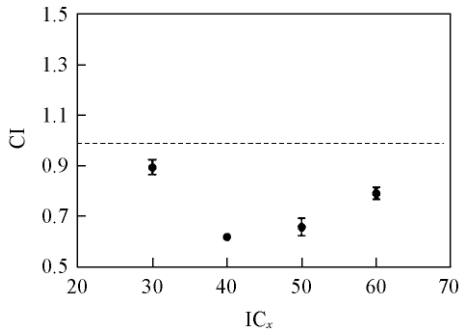

Fig.12 CI curve of MSN-Pt-PEG@Cur against Skov-3 cells after 72 h of incubation with irradiation

4 Conclusions

We have successfully developed novel light-stimulus dual-drug responsive nanoparticles based on MSN-polymer hybrid mesoporous silica. Both Cur and Pt(py) in MSN-Pt-PEG@Cur could be photoactivated by irradiation, with efficient intracellular drug release of active platinum(II) and the simultaneously generation instant ROS from Cur. Compared with the use of free anti-cancer drugs and single-drug photoactivated therapy, MSN-Pt-PEG@Cur exhibited increased photoactivated cytotoxicity. Therefore, the use of light-stimulus dual-drug responsive nanoparticles is a promising strategy for combinational photoactivated therapy.

Electronic Supplementary Material

Supplementary material is available in the online version of this article at http://dx.doi.org/10.1007/s40242-018-8077-2.

References

[1] Baek S., Singh R. K., Khanal D., Patel K. D., Lee E. J., Leong K. W., Chrzanowski W., Kim H. W., *Nanoscale,* **2015**, *7*(34), 14191

[2] Song N., Yang Y. W., *Chem. Soc. Rev.,* **2015**, *44*(11), 3474

[3] Li M., Zhang C., Yang X., *Chinese Journal of Chemistry*, **2017**, *35*(11), 1706

[4] Wang N., Tian H., Zhu S. Y., Yan D. Y., Mai Y. Y., *Chinese Journal of Polymer*, **2018**, *36*(3), 266

[5] Hou X., Zhao C., Tian Y., Dou S., Zhang X., Zhao J., *Chem. Res. Chinese Universities*, **2016**, *32*(6), 889

[6] Soenen S. J., Parak W. J., Rejman J., Manshian B., *Chem. Rev.,* **2015**, *115*(5), 2109

[7] Wang Z., Wu P., He Z., He H., Rong W., Li J., Zhou D., Huang Y., *J. Mater. B*, **2017**, *5*(36), 7591

[8] Zhang S., Qian X., Zhang D., Zhu J., Wu Y., Guo Y., Xu L., *Chem. Res. Chinese. Universities*, **2016**, *32*(1), 149

[9] Yuan Y., Kwok R. T., Zhang R., Tang B. Z., Liu B., *Chem. Commun.*, **2014**, *50*(78), 11465

[10] Lian H. Y., Hu M., Liu C. H., Yamauchi Y., Wu K. C., *Chem. Commun.,* **2012**, *48*(42), 5151

[11] Zhou D., Guo J., Kim G. B., Li J., Chen X., Yang J., Huang Y., *Adv. Healthcare Mater*., **2016**, *5*(19), 2493

[12] Lucky S. S., Soo K. C., Zhang Y., *Chem. Rev*., **2015**, *115*(4), 1990

[13] Crespy D., Landfester K., Schubert U. S., Schiller A., *Chem. Commun*., **2010**, *46*(36), 6651

[14] He S., Qi Y., Kuang G., Zhou D., Li J., Xie Z., Chen X., Jing X., Huang Y., *Biomacromolecules*, **2016**, *17*(6), 2120

[15] Ethirajan M., Chen Y., Joshi P., Pandey R. K., *Chem. Soc. Rev*., **2011**, *40*(1), 340

[16] Cong Y., Wang L., Wang Z., He S., Zhou D., Li J., Xie Z., Chen X., Jing X., Huang Y., *RSC Advances*, **2016**, *6*(24), 20366

[17] Huang P., Lin J., Wang X., Wang Z., Zhang C., He M., Wang K., Chen F., Li Z., Shen G., Cui D., Chen X., *Advanced Materials*, **2012**, *24*(37), 5104

[18] Lovejoy K. S., Lippard S. J., *Dalton Transactions*, **2009**, *38*(48), 10651

[19] Hill K. O., Fujii Y., Johnson D. C., Kawasaki B. S., *Appl. Phys. Lett*., **1978**, *32*(10), 647

[20] Meng L. B., Zhang W., Li D., Li Y., Hu X. Y., Wang L., Li G., *Chem. Commun*., **2015**, *51*(76), 14381

[21] Paschoal M. A., Tonon C. C., Spolidorio D. M., Bagnato V. S., Giusti J. S., Santos-Pinto L., *Photodiagnosis and Photodynamic Therapy*, **2013**, *10*(3), 313

[22] Scagliotti G. V., Parikh P., von Pawel J., Biesma B., Vansteenkiste J., Manegold C., Serwatowski P., Gatzemeier U., Digumarti R., Zukin M., Lee J. S., Mellemgaard A., Park K., Patil S., Rolski J., Goksel T., de Marinis F., Simms L., Sugarman K. P., Gandara D., *J. Clin. Oncol*., **2008**, *26*(21), 3543

[23] Romero-Canelon I., Sadler P. J., *Inorganic Chemistry*, **2013**, *52*(21), 12276

[24] He H., Kuang H., Yan L., Meng F., Xie Z., Jing X., Huang Y., *Physical Chemistry Chemical Physics*, **2013**, *15*(34), 14210

[25] Min Y., Li J., Liu F., Yeow E. K., Xing B., *Angew. Chem*., **2014**, *53*(4), 1012